

1.1 AN ENSEMBLE-BASED ALGORITHM TO PREDICT WARM SEASON FOG OCCURRENCE ACROSS THE HUDSON VALLEY IN EAST CENTRAL NEW YORK

Ian R. Lee*

NOAA/NWS, Weather Forecast Office, Albany, New York

1. INTRODUCTION

Hudson River Valley (Fig. 1) fogs in east central New York (NY) are often a common occurrence, typically observed within a few hours prior to sunrise. These fog events occur most frequently during the warm season months of May-October and are tied to radiational cooling effects within the planetary boundary layer (PBL). These effects are driven by variations in the static stability profile and its influence on the moisture and momentum profiles within the lowest 250 m of the PBL. Most notably, Hudson River Valley fogs are characterized by early evening (~0000 UTC) sounding profiles that exhibit an increase in the near-surface potential temperature profile coinciding with a spike in specific humidity (Acevedo and Fitzjarrald 2001, hereafter AF01). This spike in the moisture profile speeds up the saturation process and shortens the time requirement needed for fog development in the presence of a constant nighttime cooling rate (Meyer and Lala 1989, hereafter ML89). Synoptically, these fog events are promoted by a high pressure regime that supports a northerly, northwesterly, or southerly low-level moisture transport along the Hudson River Valley (ML89).

An ensemble-based algorithm is introduced utilizing a database of fog events that occurred during the 2012 and 2013 warm seasons. The algorithm compares NAM, GFS, RAP, HRRR, and WRF numerical model output, while recomputing the PBL profile from the surface to the Lifting Condensation Level (LCL) at increments based on the vertical resolution of each model. Favorability of fog development is determined through a three-step process. The first step assesses the synoptic pattern by quantitatively comparing individual model output at 925, 850, 700, 500, and 300 hPa against composite mean fields derived from NCEP/NCAR reanalysis data. The second step determines the likelihood that a PBL is supportive for fog development by quantitatively comparing the static stability, moisture, and momentum profiles from each model against observed sounding profiles.

The third step computes the time required for fog to form using an equation that relates the saturation process to the nighttime cooling rate and length of night. Final output from each model is compared to produce a probabilistic forecast of fog occurrence and onset timing.

An application of the algorithm methodology is presented from a fog event that occurred on 26 September 2014, in order to assess its role as a forecasting aid in the aviation terminal aerodrome forecast (TAF) process. This application highlights the potential benefit of this algorithm in the aviation forecasting process and in improving warm season fog forecasting across the Hudson Valley in east central NY.

2. DATA

Observational data used in the development of the algorithm include surface and upper air observations. Surface observations include 2012 and 2013 hourly METARs taken from the KALB (Albany, NY), KPOU (Poughkeepsie, NY), KPSF (Pittsfield, MA), and KGFL (Glens Falls, NY) Automated Surface Observing System (ASOS) locations (U.S. Department of Commerce 2013). Upper air observations include 0000 UTC and 1200 UTC KALB one second interval high resolution observations taken from the same time period. Composite mean fields derived from NCEP/NCAR reanalysis data (U.S. Department of Commerce 2014) are also utilized to reconstruct synoptic profiles of relative humidity (RH), geopotential height, wind speed, and wind direction at 300, 500, 700, 850, and 925 hPa, as well as mean sea level pressure (MSLP).

National Weather Service (NWS) Instrument Flight Rules (IFR) criteria (NWS Directive 10-1601) of visibility < 4.8 km (3 SM) and/or ceilings < 0.3 km (1000 ft) are used to select warm season fog events that span the months of May-October. Using this criteria, 33 fog events have been analyzed thus far with additional fog events to be added in the future. IFR events are specifically chosen for warm season fog events as they are a key NWS aviation forecasting performance metric under the Government Results and Performance Act (GPRA) ratings system (NWS Directive 10-1601).

PBL computations were calculated using a scaled, multiple subjective criteria approach. The

*Corresponding author address: Ian R. Lee, NOAA/NWS Weather Forecast Office, 251 Fuller Rd, Albany, NY, 12203. E-mail: ian.lee@noaa.gov

first criteria requires an increase in the potential temperature profile with height coinciding with a decrease in the mixing ratio profile, signifying the transition zone between the free atmosphere and friction layer (Stull 1988). The second criteria requires that the inflection point of increasing potential temperature and decreasing mixing ratio be below the LCL (i.e. cloud base). These criteria are chosen to represent the entrainment zone typically evident at the PBL capping inversion (Stull 1988). Stable nocturnal boundary layer (NBL) surface-based inversions were kept as part of the boundary layer analysis as long as a residual layer (RL) remained above it from the prior day convective boundary layer.

3. ALGORITHM COMPONENTS

The algorithm is written using the Java™ object-oriented programming language to allow for multiple platform capability (Oracle 2015). The Java capability of the algorithm also allows it to be easily integrated via a plugin with the new NWS Advanced Weather Interactive Processing System (AWIPS2) system. The algorithm analyzes BUFR model sounding output available from the NAM, NAM nest, GFS, HRRR, RAP, and WRF model run locally at the NWS Albany, NY weather forecast office. These models were chosen to provide the greatest vertical resolution of the PBL. The algorithm can easily be adapted to analyze additional model soundings as well.

The algorithm is designed to analyze BUFR model sounding output every 3 hours, primarily focusing on the 3 hour interval times between 2100-1500 UTC. Average values between 2100-1500 UTC are also computed in cases of changing weather conditions (e.g. gradually clearing sky cover). Algorithm output for each model is then averaged together to produce an ensemble-based probabilistic forecast. This approach is taken to mitigate the effects of varying model vertical resolutions and PBL physics and parameterization schemes. This approach also attempts to compensate for varying IFR fog onset times to allow for an ensemble-based average value for IFR fog onset.

4. ALGORITHM METHODOLOGY

The algorithm incorporates a three-step forecast funnel methodology, in which criteria outlined in each of the three steps must be met in order for the algorithm to predict the occurrence and potential onset of warm season IFR fog. In order for the algorithm to proceed through all three

steps, each step must meet their respective criteria. The algorithm methodology for model guidance that does not run fully through an entire analysis window (e.g. RAP, HRRR) is performed for the available analysis times only. For these instances, the algorithm outputs an alert message for model guidance that does not extend through the entire analysis window (e.g. “RAP only available through 0600 UTC – data may be unrepresentative of predicted fog occurrence”). The algorithm ends its analysis and produces a “no fog” output if one of the three steps is not met.

a) Step 1: Synoptic Favorability

The first step of the algorithm methodology assesses the synoptic favorability for warm season IFR fog and is designed with broad criteria requirements designed to narrow the field of potential warm season IFR fog environments. This first step assesses BUFR model sounding output of RH, wind speed, and wind direction at 300, 500, 700, 850, and 925 hPa and compares it against composite mean fields derived from NCEP/NCAR reanalysis data from the 33 observed fog events at 0000, 0300, 0600, 0900, and 1200 UTC. Thresholds are determined by analyzing the range from the composite fields across the Hudson River Valley and using the highest value as a filter to narrow the field of favorable synoptic patterns. Additionally, geopotential height and MSLP are compared to narrow the analysis to warm season fog events in favorable high pressure regimes (Fig. 2). Table 1 outlines the criteria that must be met during the first step of the algorithm methodology. If any of the criteria are not met, the algorithm produces output that states that the synoptic setup is not favorable for fog formation and describes why (e.g. “500 hPa geopotential height too low”). If the criteria outlined in Table 1 are not met, the algorithm will not continue further.

Summarizing Table 1, relatively dry and weak upper-level synoptic flow is favored above 850 hPa, with relatively moist and weak low-level flow below 850 hPa. Low-level wind trajectories are favored either from the south/southeast (Hudson River), west/northwest (Mohawk River), or north/northeast (Lake Champlain) to allow for moisture advection off these local sources of water (Fig. 1). High pressure regimes are also favored synoptically, as they are often associated with conditions commonly synonymous with fog formation (e.g. clear skies, light winds). Figure 3 depicts a conceptual model of the first step in the algorithm methodology.

b) Step 2: PBL Favorability

The second step of the algorithm methodology assesses the PBL favorability of the stability, moisture, and momentum profiles. Each profile analyzed during this step is evaluated based on the profile trend and not by geographical location (Fig. 4). The stability profile is assessed by first evaluating the depth of the PBL (i.e. LCL height) in relation to turbulent mixing potential (Figs. 5, 6). Shallow PBL depths are favored in order to inhibit the growth of large, vertically-oriented turbulent eddies that increase PBL mixing and dry air entrainment (Oke 1978). The strength of the PBL capping inversion is also taken into consideration to assess the degree to which entrainment effects are limited. To categorize PBL stability as a whole, the algorithm computes the potential temperature profile. Most notably, the algorithm computes the potential temperature difference between the surface and 250 m at 0000 UTC, and between the surface and 500 m at 0300, 0600, 0900, and 1200 UTC. The difference in height is increased for the nighttime hours to allow for growth of the NBL (Stull 1988). Potential temperature profiles increasing with height between these layers are favored indicating a stable stability profile (Stull 1991). Stable profiles are preferred as they influence the trapping of moisture and inhibit turbulence production (Stull 1988; 1991). The depth of the stable NBL is used by the algorithm as a proxy for IFR ceiling height and is computed by calculating where the NBL surface-based potential temperature inversion decreases with height (i.e. onset of RL).

The moisture profile is assessed by evaluating the mixing ratio, specific humidity (q), and RH profiles. RH and q are computed via the model temperature, dewpoint, and mixing ratio profiles. The mean PBL mixing ratio and RH are assessed to determine if enough moisture is present for fog formation. Similar to the potential temperature profile, the algorithm computes the specific humidity and RH difference between the surface and 250 m at 0000 UTC, and between the surface and 500 m at 0300, 0600, 0900, 1200 UTC. At 0000 UTC, the algorithm assesses whether there is an increasing profile in both q and RH in order to capture moisture trapping as part of the Early-Evening Surface Layer Transition (EET) that typically occurs near sunset (AF01).

The EET (Fig. 7) occurs when the loss of daytime heating, and subsequent thermally-driven turbulent mixing, decreases near-surface wind speeds and allows for the onset of the stable NBL (AF01). This stable NBL is initially within the lowest 250 m above the surface, evident by an increasing static stability (potential temperature) profile that

allows moisture to be trapped near the surface (AF01). The algorithm evaluates for these increasing q and RH profiles at 0000 UTC as this moisture trapping accelerates the nighttime saturation process required for fog formation (AF01).

At 0300, 0600, 0900, and 1200 UTC, the algorithm assesses if the q profile remains increasing with height between the surface and 500 m to signify moisture being trapped near the surface. At these same analysis times, the algorithm assesses if the RH profile is decreasing with height to signify weak mixing in the NBL and condensation of rising water droplets versus negligible mixing and settling of water droplets and resultant dew formation. An increasing RH profile may be an indicator of deeper NBL mixing and resultant low stratus formation.

The momentum profile is assessed by evaluating the wind speed, wind direction, and the Bulk Richardson Number (R_i). The algorithm calculates the PBL mean wind speed and compares the subgeostrophic and supergeostrophic (if present) components in the PBL to assess entrainment effects (Stull 1988; Banta et al. 2002). The algorithm uses a mean wind value 2.5 m/s (5 kt) less than the 925 hPa wind criteria (Table 1) to account for frictional effects within the PBL. Wind direction is favored either up the Hudson Valley from the south/southeast (150°-190°), down the Mohawk Valley from the west/northwest (270°-320°), or downwind of Lake Champlain from the north/northeast (350°-040°) in order to allow for PBL moisture advection (Figs. 1 and 3).

The algorithm computes the R_i using the following equation as defined in Stull 1988:

$$R_i = \frac{g \frac{\partial \theta}{\partial z}}{\theta \frac{\partial u^2}{\partial z}} \quad (1)$$

Where:

g = gravity (9.8 m/s²)

$\frac{\partial \theta}{\partial z}$ = vertical potential temperature gradient

θ = average layer potential temperature

$\frac{\partial u}{\partial z}$ = vertical wind shear gradient

The R_i is used as an estimate to assess turbulent mixing potential within the PBL (Stull 1988). The algorithm uses a critical R_i of 0.25 and a R_i value of 0.00 to differentiate between PBLs that support turbulent mixing ($R_i < 0.00$), dampen turbulent mixing (R_i 0.00-0.25), and suppress

turbulent mixing $R_i \geq 0.25$). The algorithm requires a mean PBL R_i profile > -0.10 at 2100 UTC and > 0.00 at 0000, 0300, 0600, 0900, and 1200 UTC. The algorithm also requires at least one layer between the surface and 500 m to be ≥ 0.25 in order to assess the potential for suppressed mixing near the surface.

Additionally, mean PBL temperature is also computed to limit PBLs to the warm season. Table 2 outlines the criteria that must be met during the second step of the algorithm methodology. Summarizing Table 2, highly stable, moist and low momentum PBLs are favored for warm season IFR fog formation. Figure 8 depicts a conceptual model of the second step in the algorithm methodology. If any of the criteria outlined in Table 2 or Figure 8 are not met, the algorithm produces output that states that the boundary layer setup is not favorable for fog formation and describes why (e.g. "potential temperature too favorable for mixing"). If the criteria outlined in Table 2 and Figure 8 are not met, the algorithm will not continue further.

c) Step 3: Surface Favorability

The third step of the algorithm methodology assesses the surface favorability with respect to the nighttime cooling rate and length of night (LON). The algorithm assesses the surface variability by assessing the surface temperature, dewpoint, dewpoint depression, RH, and wind speed (Table 3). Wind direction is not used as part of the surface variability assessment due to effects caused by objects (e.g. buildings, trees, etc.) and local circulations.

The cooling rate τ (Tau) is defined as the cooling rate between 0000-0400 UTC using the following equation from ML89:

$$\tau \approx \frac{\frac{RT^2}{\epsilon L_v} \ln(RH_o)}{\frac{\partial T}{\partial t}} \quad (2)$$

Where:

R = dry gas constant for air (287 J K⁻¹ kg⁻¹)

T = 0000 UTC temperature (K)

ϵL_v = latent heat of vaporization x 0.622 (constant value of 1523900 kJ/kg)

RH_o = 0000 UTC RH (decimal form)

$\frac{\partial T}{\partial t}$ = 0000-0400 UTC cooling rate (K/hr)

The output value for Tau is positive (assuming cooling between 0000-0400 UTC) and is compared against the average value of LON (Table 4) for each month (ML89). If the value of Tau is less than the

monthly LON value, the LON is long enough to allow the nighttime saturation process to complete and for fog formation to occur (ML89). If the value of Tau is greater, the nighttime saturation process will not complete as the LON is too short (ML89). If the compared value of Tau against LON is negative, the algorithm then subtracts the Tau value from 1200 UTC (i.e. ~sunrise) to estimate the onset time of fog formation. Positive values will not result in an algorithm prediction of fog formation as either the nighttime cooling rate or LON is not favorable.

5. APPLICATION – 26 SEPTEMBER 2014

An application of the algorithm methodology as a forecasting aid in the NWS aviation TAF forecast process at KALB (Albany, NY) is presented for an observed warm season IFR fog event that occurred during the early morning hours (0600-1200 UTC) of 26 September 2014. This application utilizes BUFR model sounding output from the NAM nest valid at 1800 UTC 25 September 2014. Table 5 outlines the model sounding output for assessing the synoptic favorability of the algorithm methodology (Step 1). The output indicates a favorable high pressure regime with light low-level winds, ample low-level moisture, and decreasing upper-level moisture. With light winds, ample low-level moisture and decreasing upper-level moisture indicative of gradually clearing sky cover, the synoptic conditions are favorable for potential fog formation and meet the criteria outlined in Step 1 of the algorithm methodology (Table 1).

Table 6 outlines the model sounding output for assessing the PBL favorability of the algorithm methodology (Step 2). In addition to a favorable synoptic pattern, the PBL profile is also supportive for fog formation. The relatively shallow PBL is characterized by highly stable, moist, and low momentum profiles evident by the predicted occurrence of an EET at 0000 UTC and a supportive stable NBL between 0000-1200 UTC. Given these PBL profiles, the PBL is supportive of potential fog formation if the saturation process can complete.

Assessing the surface favorability of the algorithm methodology (Step 3), the surface meets the criteria outlined in Table 3 (not shown). With this fog event occurring in September, an average value for the LON of 11.48 (Table 4) is used with a model-depicted 0000-0400 UTC cooling rate of -0.7 K/hr. Plugging the cooling rate of -0.7 K/hr into Eqn. (2) with a model-depicted 0000 UTC temperature of 299 K and RH of 0.80 produces an output value for Tau of 5.37. Since this value of Tau is less than the

average September LON value, fog formation is possible given the favorable synoptic pattern and PBL profiles. To estimate the possible onset time of fog formation, the algorithm subtracts Tau from 1200 UTC to produce a predicted fog formation onset time of ~0600 UTC. This predicted fog formation onset time matches to the actual observed value providing confidence that this particular model was accurately predicting IFR fog. This final output of the algorithm methodology could then be used to introduce a period of IFR fog into the KALB TAF beginning at 0600 UTC if other sources of model guidance produced similar algorithm output.

6. DISCUSSION

An ensemble-based algorithm to predict warm season IFR fog occurrence across the Hudson Valley is introduced. The algorithm incorporates a forecast funnel methodology that assesses the synoptic, PBL, and surface favorability for warm season IFR fog formation. Highly stable, moist, and low momentum PBLs are favored with weak and relatively dry synoptic flow amidst a high pressure regime. A nighttime cooling rate aided by an EET is favored as it accelerates the nighttime saturation process. A sufficient LON is required to allow for the saturation process to complete. Precipitation can potentially increase the likelihood of fog formation, but is not required if low-level flow trajectories promote moisture advection via the Hudson Valley, Mohawk Valley, or Lake Champlain.

The algorithm assesses PBL variability by treating PBL profiles as profile-relative and not by geographic location. This analysis allows for evaluation of common PBL profile trends favorable for warm season IFR fog which may be applicable to additional sites outside of the Hudson Valley. The synoptic favorability, however, can only be applied locally to the Hudson Valley and additional research is needed to develop other local geographic preferences.

By incorporating more advanced PBL physics favorable for fog formation, the algorithm presented in this paper may improve forecasting of IFR warm season fog in the Hudson Valley. Additionally, incorporating multiple sources of model guidance, each with varying degrees of vertical resolution and PBL physics and parameterization schemes, the algorithm presented in this paper offers a probabilistic output of warm season IFR fog potential similar to other methods discussed in the literature (Roquelaure and Bergot 2009; Binbin and Du 2010). The probabilistic nature of the algorithm

allows for an ensemble-based approach to fog forecasting that may minimize the limitations of fog prediction associated with various sources of deterministic model guidance.

7. FUTURE WORK

The algorithm presented in this paper is planned to undergo testing in an operational environment during the 2015 warm season in order to assess real-time performance and verification. A comparison of BUFR model soundings to observed warm season IFR fog event soundings is also planned in order to assist in developing additional NWS aviation forecast aids. Future algorithm iterations are also planned to incorporate real-time surface observations and further advanced PBL physics (e.g. flux calculations), as well as predictions for fog intensity and dissipation times. Finally, NWS Graphical Forecast Editor (GFE) Smart Tools using the concepts discussed in this paper may also be developed in the future to aid operational forecasters.

8. ACKNOWLEDGMENTS

The author would like to thank Dr. Dave Fitzjarrald and Dr. Jeff Freedman from SUNY Albany Atmospheric Sciences Research Center for their invaluable insight and continued support of this research.

The author also thanks ALY Science Operations Officer, Warren R. Snyder, ALY Meteorologist In Charge Raymond G. O'Keefe, ALY Warning Coordination Meteorologist Stephen DiRienzo, ALY Information Technology Officer Vasil Koleci, ALY forecasters Tom Wasula, Joe Villani, Kevin Lipton, and Neil Stuart, and Brian Miretzky from Eastern Region Scientific Services Division for reviewing this extended manuscript publication. The author would also like to acknowledge the CSTAR V program (Grant #: NA13NWS4680004).

DISCLAIMER

Reference to any specific commercial products, process, or service by trade name, trademark, manufacturer, or otherwise, does not constitute or imply its recommendation, or favoring by the United States Government or NOAA/National Weather Service. Use of information from this

publication shall not be used for advertising or product endorsement purposes.

9. REFERENCES

- Acevedo O. C., and D. R. Fitzjarrald, 2001: The Early Evening Surface-Layer Transition: Temporal and Spatial Variability. *J. Atmos. Sci.*, 58, 2650–2667.
- Banta, R. M., R. K. Newsom, J. K. Lundquist, Y. L. Pichugina, R. L. Coulter, and L. J. Mahrt, 2002: Nocturnal low-level jet characteristics over Kansas during CASES-99. *Bound.-Layer Meteor.*, 105, 221–252.
- Fitzjarrald D. R., and G. G. Lala, 1989: Hudson Valley Fog Environments. *J. Appl. Meteor.*, 28, 1303–1328.
- Meyer M.B., and G.G. Lala, 1989: Climatological aspects of radiation fog occurrence at Albany, New York. *J. Climate*. 3, 577-586.
- NOAA/NWS, Cited 2014: NWS Directives 10-1601 Verification. [Available online at: <http://www.nws.noaa.gov/directives/sym/pd01016001curr.pdf>]
- Oke, T.R., 1978: *Boundary Layer Climates*, Halsted Press, 372 pp.
- Oracle, Cited 2014. [Available online at: <http://www.oracle.com/technetwork/java/javase/documentation/index.html>]
- Roquelaure S., and T. Bergot, 2009: Contributions from a Local Ensemble Prediction System (LEPS) for Improving Fog and Low Cloud Forecasts at Airports. *Wea. Forecasting*, 24, 39–52.
- Stull, R.B., 1988: *An Introduction to Boundary Layer Meteorology*. Volume 13. Kluwer Academic Publishers, 670 pp.
- Stull, R.B., 1991: Static Stability - An Update. *Bull. Amer. Meteorol. Soc.* 72, 1521-1529.
- U.S. Department of Commerce/National Climatic Data Center, Cited 2013. [Available online at: <http://www.ncdc.noaa.gov/data-access/landbased-station-data/land-based-datasets/quality-controlled-local-climatological-data-qclcd>]
- U.S. Department of Commerce/Earth Systems Research Laboratory Physical Sciences Division NCAR Reanalysis, Cited 2014. [Available online at: <http://www.esrl.noaa.gov/psd/data/composites/day>]
- Zhou B., and J. Du, 2010: Fog Prediction from a Multimodel Mesoscale Ensemble Prediction System. *Wea. Forecasting*, 25, 303–322.

| Pressure Level (hPa) | RH (%) | Geopotential Height | Wind Speed (kt) | Wind Direction (°) |
|----------------------|--------|---------------------|-----------------|---------------------------|
| 300 | < 70 | N/A | N/A | N/A |
| 500 | < 70 | 556-592 dam | N/A | N/A |
| 700 | < 70 | 297-325 dam | N/A | N/A |
| 850 | > 50 | 140-162 dam | < 40 | 150-190, 270-320, 350-040 |
| 925 | > 50 | 704-902 m | < 30 | 150-190, 270-320, 350-040 |
| MSLP > 1004 hPa | > 50 | N/A | < 6 | N/A |

Table 1: Synoptic criteria for Step 1 of the algorithm methodology. Criteria valid at 0000, 0300, 0600, 0900, and 1200 UTC.

| Criteria | 2100 UTC | 0000 UTC | 0300, 0600, 0900, 1200 UTC |
|--|----------|----------|----------------------------|
| LCL height (m) | < 2000 | < 2000 | < 2000 |
| Mean wind speed (kt) | < 25 | < 25 | < 25 |
| Mean wind direction (°) | N/A | N/A | 150-190, 270-320, 350-040 |
| Mean RH (%) | > 40 | > 40 | > 60 |
| Mean temperature (°C) | 5-25 | 5-25 | 5-25 |
| Mean Bulk Richardson Number | > -0.10 | > 0.00 | > 0.00 |
| Mean Mixing Ratio (g/kg) | > 2 | > 2 | > 2 |
| Top of PBL inversion strength (≥ 0.2 °C) | N/A | 0.2 | 0.2 |

- **0000 UTC:** Positive change in height between surface and 250 m with specific humidity/potential temperature \longrightarrow Early Evening Surface Layer Transition (EET)
- RH value at 250 m greater than surface
- **0300, 0600, 0900, 1200 UTC:** RH value at 500 m less than surface (greater = low stratus)
- **0000, 0300, 0600, 0900, 1200 UTC:** Bulk Richardson Number ≥ 0.25 between surface and 500 m

Table 2: PBL criteria for Step 2 of the algorithm methodology.

| Temperature (°C) | Dewpoint (°C) | Dewpoint Depression (°C) | RH (%) | Wind Speed (kt) |
|------------------|---------------|--------------------------|--------|-----------------|
| 5-30 | 0-25 | < 12 | > 45 | < 6 |

Table 3: Surface criteria for Step 3 of the algorithm methodology. Criteria valid at 2100, 0000, 0300, 0600, 0900, 1200 UTC.

| Month | Average Length of Night |
|-----------|-------------------------|
| January | 14.57 |
| February | 13.47 |
| March | 12.08 |
| April | 10.62 |
| May | 9.38 |
| June | 8.74 |
| July | 9.02 |
| August | 10.09 |
| September | 11.48 |
| October | 12.93 |
| November | 14.21 |
| December | 14.91 |

Table 4: Average monthly LON values computed for the Hudson Valley (ML89).

| Time | 0000 UTC | 0300 UTC | 0600 UTC | 0900 UTC | 1200 UTC | Average |
|---|-----------------|-----------------|-----------------|-----------------|-----------------|-----------------|
| 300 RH (%) | 62 | 69 | 52 | 58 | 19 | 52 |
| 500 Height (dam)/RH (%) | 571/66 | 571/66 | 570/47 | 570/2 | 572/9 | 571/38 |
| 700 Height (dam)/RH (%) | 316/19 | 316/15 | 315/10 | 315/5 | 315/14 | 315/63 |
| 850 Height (dam)/RH (%) / wind (kt) | 157/17/6 | 157/4/11 | 156/11/17 | 156/56/20 | 156/57/17 | 156/29/14 |
| 925 Height (m)/RH (%) / wind (kt) | 861/68/5 | 860/70/11 | 858/72/12 | 856/79/17 | 856/88/17 | 858/75/12 |
| Surface MSLP (hPa)/RH (%) / wind dir. (degrees) | 1013/79/ 355 | 1012/77/ 330 | 1012/79/ 298 | 1012/93/ 315 | 1012/90/ 319 | 1012/84/ 323 |

Table 5: NAM nest output valid 25 September 2014 of Step 1 algorithm criteria at 0000, 0300, 0600, 0900, and 1200 UTC. Green shading indicates values that fall within Table 1 criteria.

| Time | 2100 UTC | 0000 UTC | 0300 UTC | 0600 UTC | 0900 UTC | 1200 UTC | Average |
|--|-------------|-------------|-------------|-------------|-------------|-------------|---------|
| LCL height (m) – must be below 2000 m | 1140 | 865 | 610 | 555 | 500 | 505 | 696 |
| Mean wind speed (kt)/direction (degrees) | 3/30 | 6/52 | 8/37 | 8/360 | 7/330 | 7/355 | 7/13 |
| Mean RH (%) | 69 | 70 | 66 | 68 | 83 | 88 | 74 |
| Mean temperature (°C) | 15 | 15 | 15 | 15 | 13 | 12 | 14.2 |
| Mean Bulk Richardson Number | -0.04 | 0.03 | 0.21 | 0.31 | 0.27 | 0.25 | 0.17 |
| Top of PBL inversion strength (≥ 0.2 °C) | N/A | 0.3 | 0.4 | 0.6 | 0.9 | 0.8 | 0.6 |

- **00 UTC:** Positive change in height between surface and 250 m with specific humidity/potential temperature – YES → Early Evening Surface Layer Transition (EET) predicted
- RH value at 250 m greater than surface – YES
- **03, 06, 09, 12 UTC:** RH value at 500 m less than surface (greater = low stratus) – YES
- **00, 03, 06, 09, 12 UTC:** Bulk Richardson Number ≥ 0.25 between surface and 500 m – YES

Table 6: NAM nest output valid 25 September 2014 of Step 2 algorithm criteria at 2100, 0000, 0300, 0600, 0900, and 1200 UTC. Green shading indicates values that fall within Table 2 criteria. Criteria labeled “YES” below table indicate model prediction of EET (AF01).

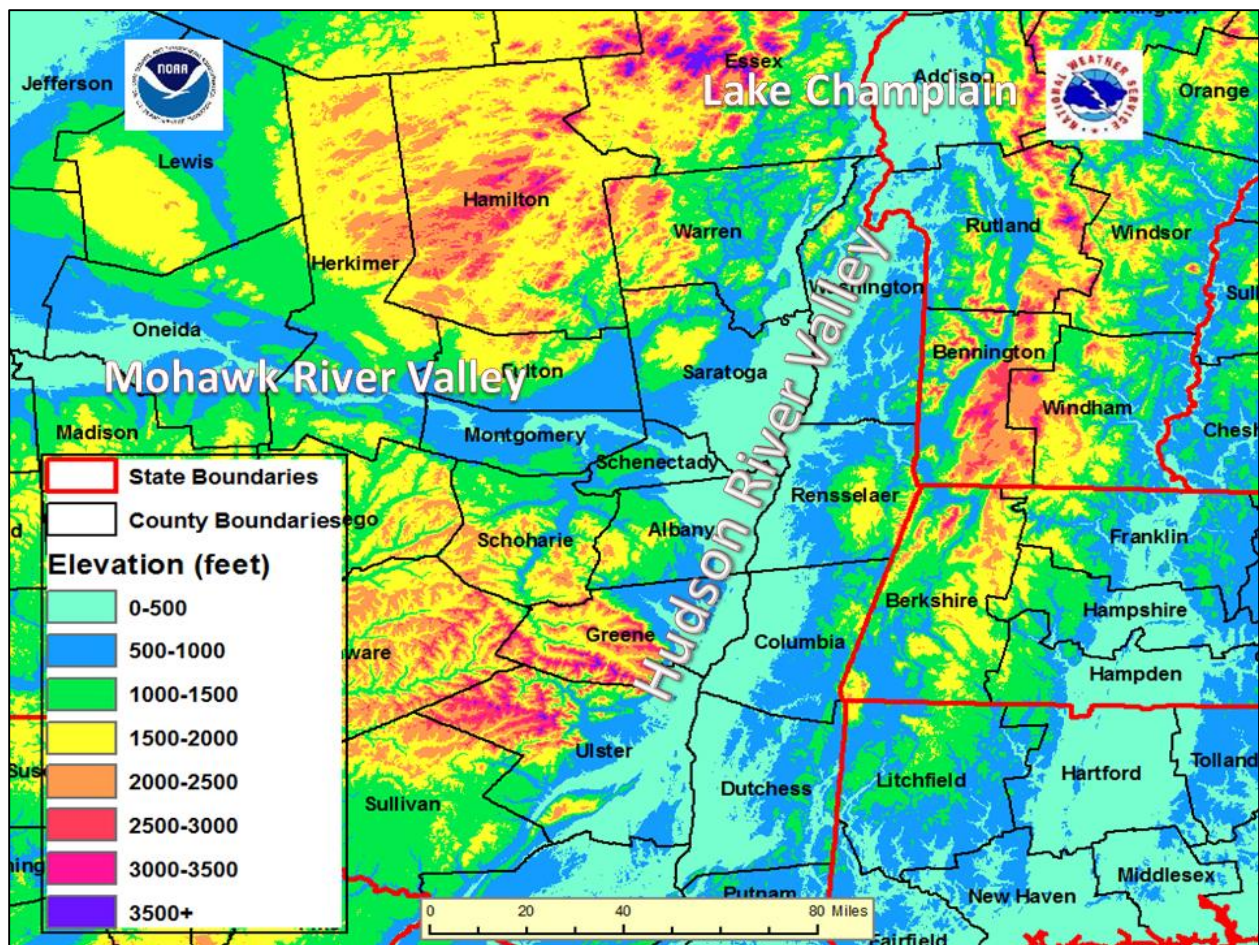


Figure 1: Topographic map of the Hudson Valley in east central NY.

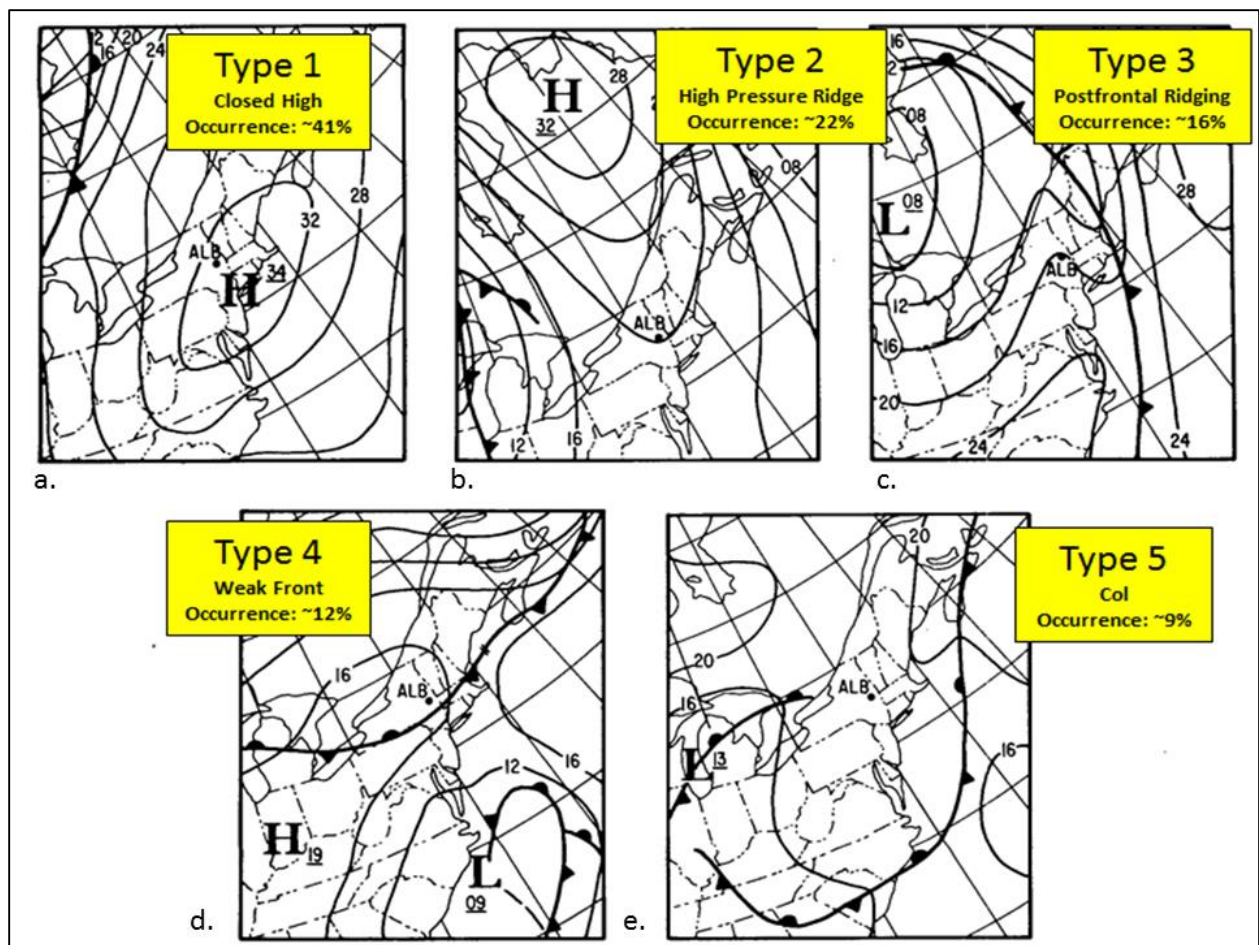


Figure 2: Most common climatological surface pressure regimes for Hudson Valley fogs. Adapted from ML89.

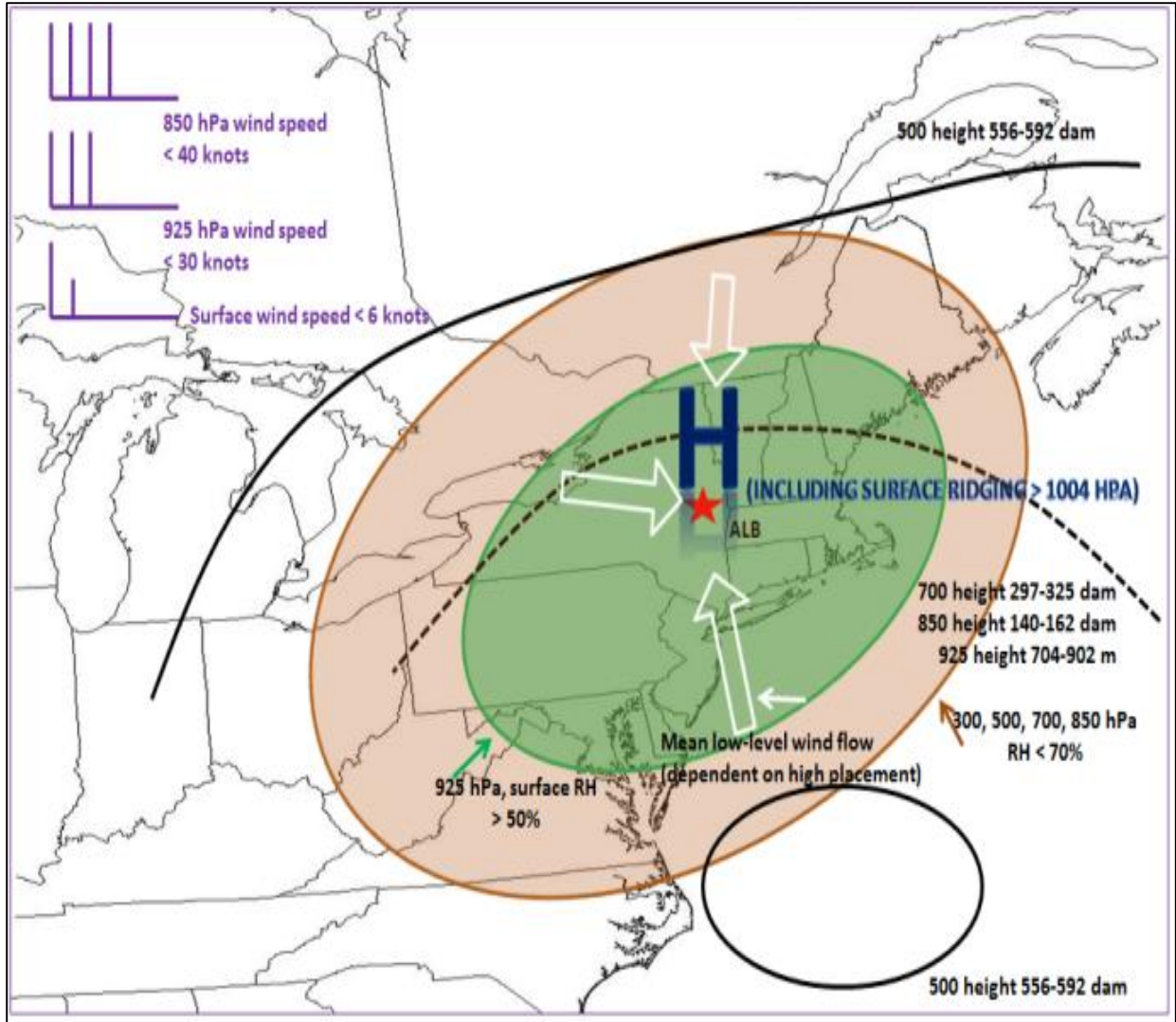


Figure 3: Conceptual model of the synoptic favorability (Step 1) algorithm methodology.

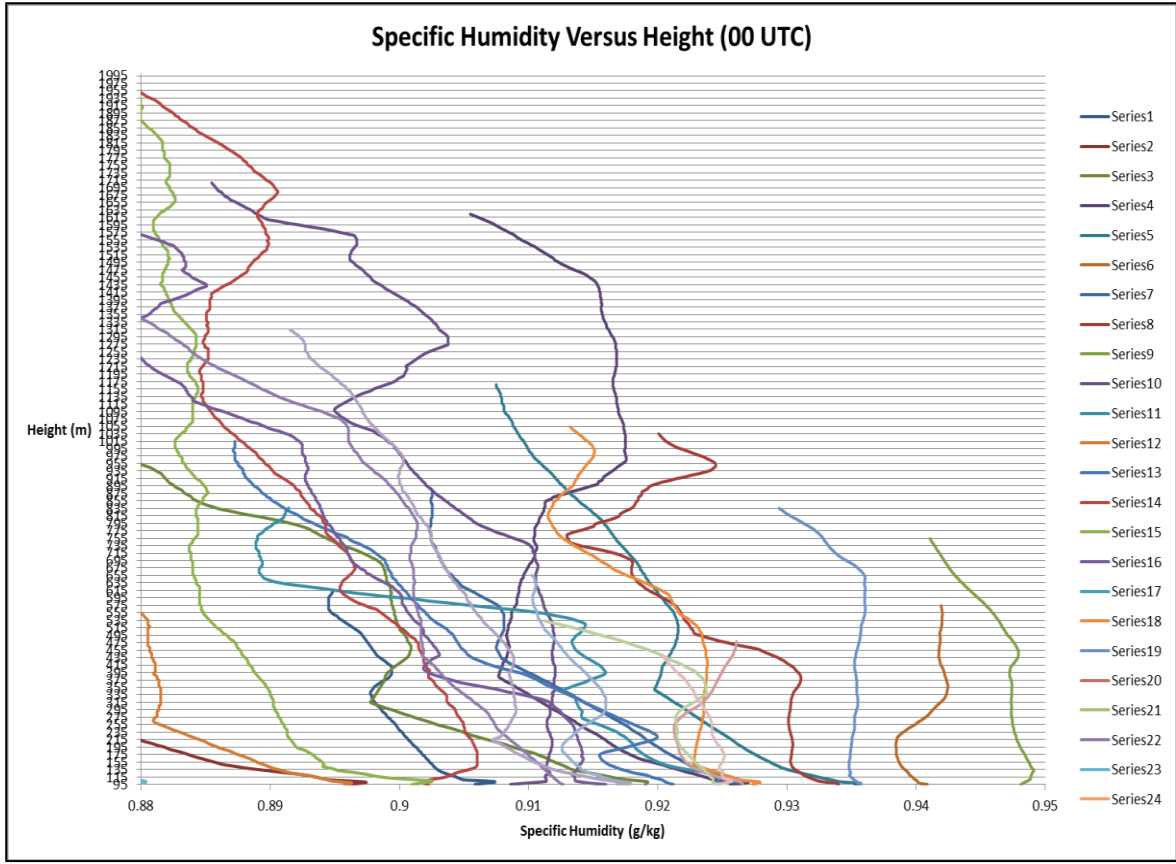


Figure 4: Example of PBL profile-relative analysis as part of Step 2 algorithm methodology.

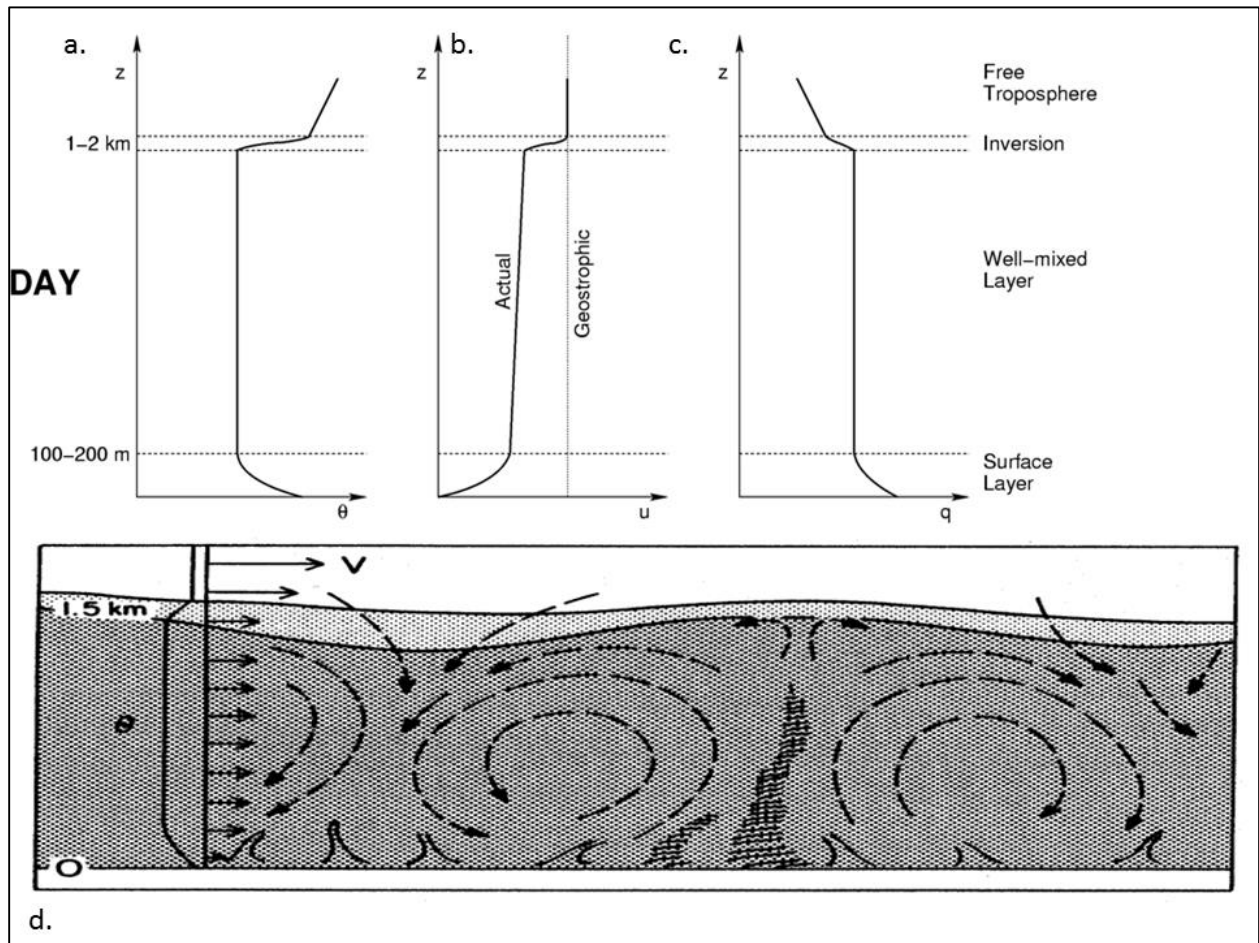


Figure 5: Typical daytime PBL profile of potential temperature (a), wind speed (b), specific humidity (c), and turbulence distribution (d). Adapted from Stull 1988.

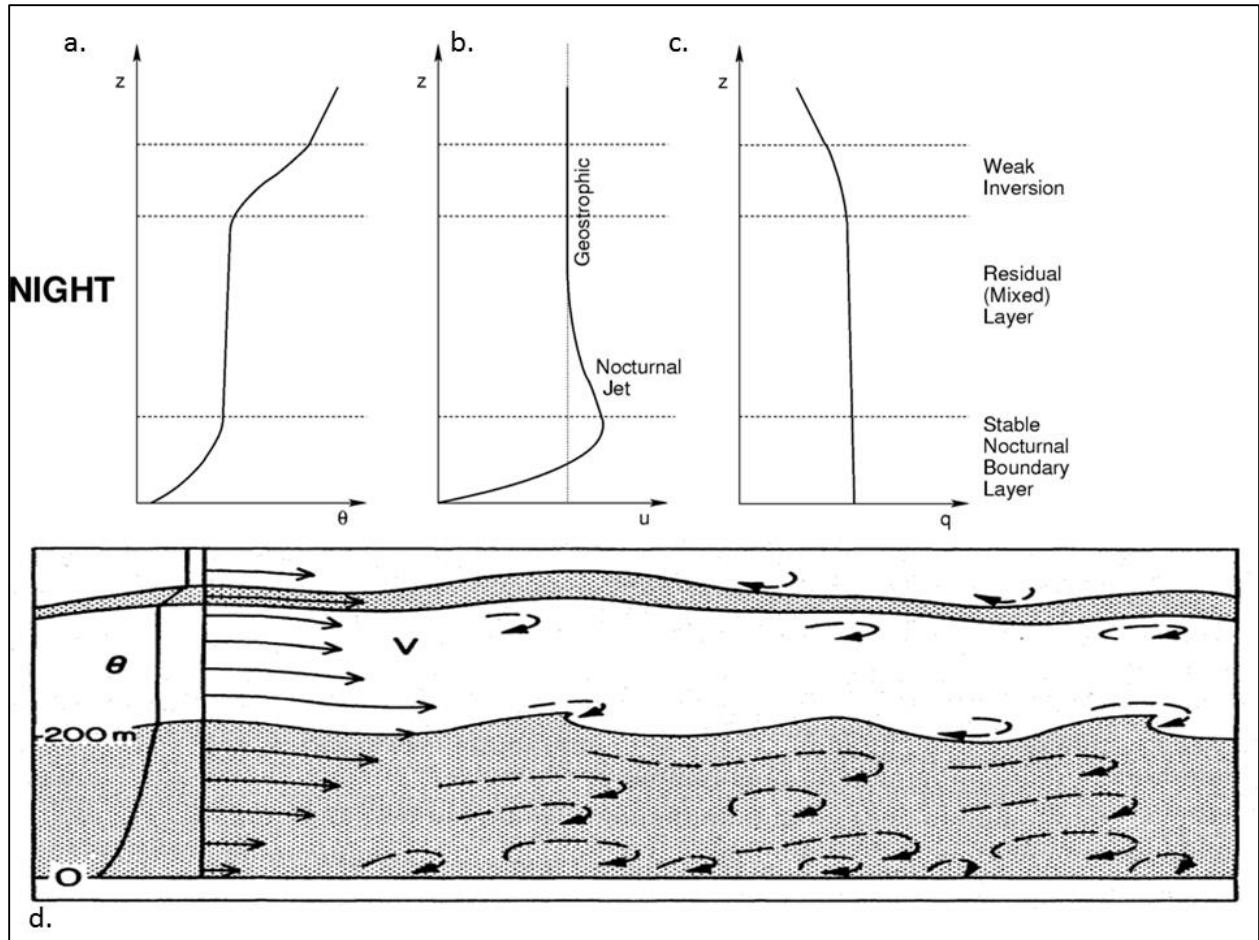


Figure 6: Typical nighttime PBL profile of potential temperature (a), wind speed (b), specific humidity (c), and turbulence distribution (d). Adapted from Stull 1988.

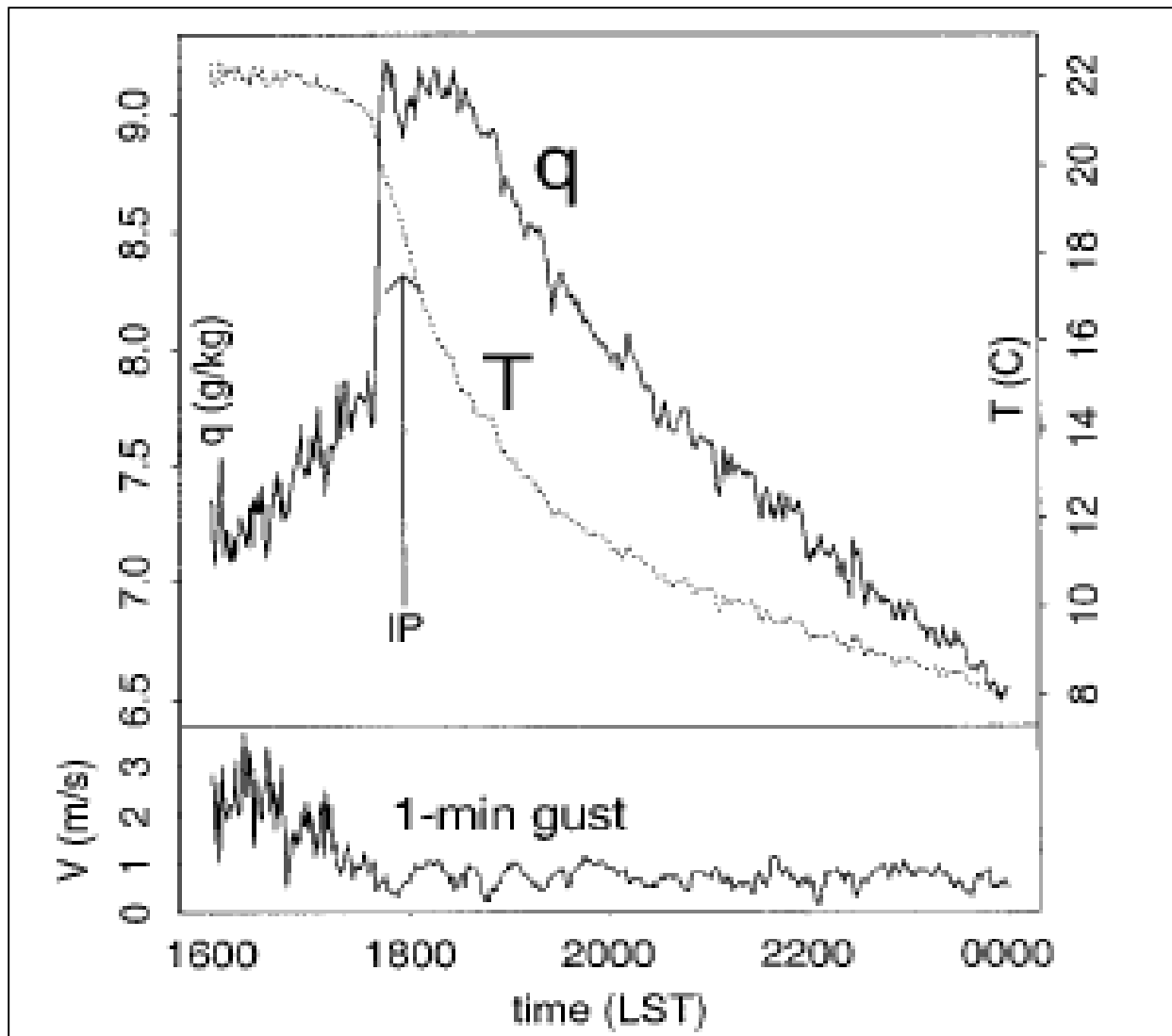


Figure 7: EET profiles of temperature (T), specific humidity (q), and wind speed (1-min gust). Adapted from AF01.

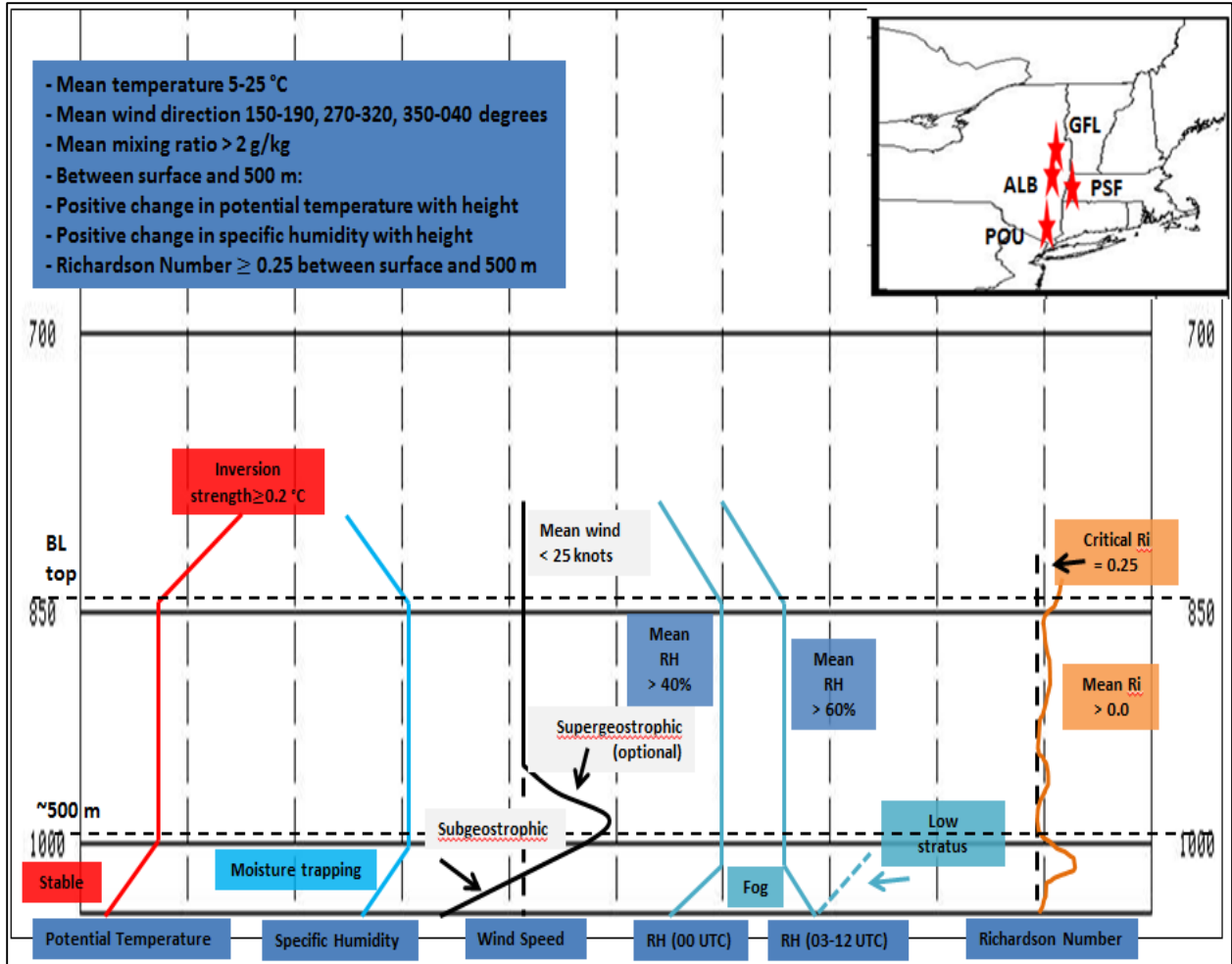


Figure 8: Conceptual model of the PBL favorability (Step 2) algorithm methodology.